Small Ca^{2+} releases enable hour-long high-frequency contractions in midshipman swimbladder muscle

Frank E. Nelson,[1,4,5] Stephen Hollingworth,[2] James O. Marx,[3] Stephen M. Baylor,[2] and Lawrence C. Rome[1,4]

[1]Department of Biology, [2]Department of Physiology, Perelman School of Medicine, and [3]Department of Pathobiology, School of Veterinary Medicine, University of Pennsylvania, Philadelphia, PA
[4]The Whitman Center, Marine Biological Laboratory, Woods Hole, MA
[5]Department of Biology, Temple University, Philadelphia, PA

Type I males of the Pacific midshipman fish (*Porichthys notatus*) vibrate their swimbladder to generate mating calls, or "hums," that attract females to their nests. In contrast to the intermittent calls produced by male Atlantic toadfish (*Opsanus tau*), which occur with a duty cycle (calling time divided by total time) of only 3–8%, midshipman can call continuously for up to an hour. With 100% duty cycles and frequencies of 50–100 Hz (15°C), the superfast muscle fibers that surround the midshipman swimbladder may contract and relax as many as 360,000 times in 1 h. The energy for this activity is supported by a large volume of densely packed mitochondria that are found in the peripheral and central regions of the fiber. The remaining fiber cross section contains contractile filaments and a well-developed network of sarcoplasmic reticulum (SR) and triadic junctions. Here, to understand quantitatively how Ca^{2+} is managed by midshipman fibers during calling, we measure (a) the Ca^{2+} pumping-versus-pCa and force-versus-pCa relations in skinned fiber bundles and (b) changes in myoplasmic free [Ca^{2+}] ($\Delta[Ca^{2+}]$) during stimulated activity of individual fibers microinjected with the Ca^{2+} indicators Mag-fluo-4 and Fluo-4. As in toadfish, the force–pCa relation in midshipman is strongly right-shifted relative to the Ca^{2+} pumping–pCa relation, and contractile activity is controlled in a synchronous, not asynchronous, fashion during electrical stimulation. SR Ca^{2+} release per action potential is, however, approximately eightfold smaller in midshipman than in toadfish. Midshipman fibers have a larger time-averaged free [Ca^{2+}] during activity than toadfish fibers, which permits faster Ca^{2+} pumping because the Ca^{2+} pumps work closer to their maximum rate. Even with midshipman's sustained release and pumping of Ca^{2+}, however, the Ca^{2+} energy cost of calling (per kilogram wet weight) is less than twofold more in midshipman than in toadfish.

INTRODUCTION

In certain fish species that live in turbid waters, male fish vibrate their gas-filled swimbladder to generate calls that attract females for mating. In one such fish, the Atlantic toadfish (*Opsanus tau*), the swimbladder muscles can contract and relax at up to 100 Hz at 15°C and 250 Hz at 25°C. To activate and relax at these high frequencies, which correspond to the frequencies of the generated sound, the superfast fibers of the swimbladder muscles require several kinetic specializations, including (a) the briefest myoplasmic free Ca^{2+} transient ever measured; (b) a troponin isoform with a low affinity for Ca^{2+}, which probably arises because of an unusually fast off-rate constant for Ca^{2+}; and (c) a myosin isoform with the fastest known rate constant for cross-bridge detachment (Rome et al., 1996, 1999a; Rome, 2006).

A challenging design issue associated with the generation of these mating calls relates to the handling of Ca^{2+}, whose changes in myoplasmic concentration control the fiber contractions. If, with each fiber action potential (AP), the SR releases sufficient Ca^{2+} to saturate the Ca^{2+}-regulatory sites on troponin, then the measured rate of Ca^{2+} pumping in toadfish is insufficient to recycle all of the released Ca^{2+} back to the lumen of the SR before the next stimulus (Young et al., 2003). Toadfish have solved this Ca^{2+} problem in two ways. First, toadfish reduce the amount of Ca^{2+} released so that, during most twitches in a call, less than 50% of the troponin regulatory sites become Ca^{2+} bound in response to each AP (Harwood et al., 2011). Second, toadfish do not fully recycle Ca^{2+} to the SR with each AP; rather, as the call progresses, 70–80% of the released Ca^{2+} becomes bound by parvalbumin (Parv), a soluble Ca^{2+}-binding protein that is found in toadfish at the highest concentrations ever measured (Tikunov and Rome, 2009). An important behavior associated with this design strategy is that toadfish, which can call repetitively for many hours, do so with a 3–8% "duty cycle," in which brief 400–500-ms periods of sound production are interleaved with relatively long 5–15-s silent periods, or "intercall intervals" (Edds-Walton et al., 2002). Parv, which is nearly saturated with Ca^{2+} by the end of an individual call, releases its Ca^{2+} slowly during the long intercall interval as Ca^{2+}

Correspondence to Lawrence C. Rome: lawrence.rome@gmail.com

The Rockefeller University Press
J. Gen. Physiol. 2018 Vol. 150 No. 1 127–143
https://doi.org/10.1085/jgp.201711760

is pumped back into the SR in preparation for the next call (Nelson et al., 2014).

In striking contrast to toadfish, the type I male of another fish species, the Pacific midshipman (*Porichthys notatus*), makes its mating call with a 100% duty cycle and can do so for up to an hour (12–16°C). With the swimbladder vibrating continuously at 50–100 Hz, the result can be as many as 360,000 muscle contractions in an hour (Brantley et al., 1993; Bass et al., 1999). Without an intercall interval to unload bound Ca^{2+} from Parv, the Parv mechanism cannot be useful, and accordingly, the amount of Parv per wet weight in midshipman fibers is only one-eighth that in toadfish fibers (Tikunov and Rome, 2009). The question then remains: how does midshipman manage its Ca^{2+} during 100% duty cycle calls?

Two general Ca^{2+} strategies might be used for 100% duty cycle calling. First, midshipman fibers might have more and/or faster SR Ca^{2+} pumps than toadfish fibers. Second, if the number and function of Ca^{2+} pumps in midshipman fibers is similar to that in toadfish fibers, the amount of SR Ca^{2+} released per stimulus might be considerably less than in toadfish. In nature's most extreme case of repetitive muscle action, the high frequency asynchronous flight muscles of insects release virtually no Ca^{2+} on each force and work cycle (Josephson et al., 2000).

Here we show that type I male midshipman swimbladder fibers stimulated at 67–100 Hz at 16°C produce a Ca^{2+} and force transient with each stimulus, indicating that midshipman use high-frequency synchronous, not asynchronous, contractions. We also find that the maximum rate of Ca^{2+} pumping in midshipman, although high, is actually lower than in toadfish. Further, we show that the amplitude of the Ca^{2+} transient in midshipman is only 10–20% that in toadfish, and our computational modeling indicates that the amount of SR Ca^{2+} release per twitch in the myofibrillar region of the fiber is only approximately one-eighth that in toadfish. Thus, despite a 20-fold larger duty cycle, midshipman swimbladder fibers release less than twofold more Ca^{2+} per kilogram wet weight during calling than toadfish swimbladder fibers. The larger release does require faster average Ca^{2+} pumping, and this is achieved because the higher average myoplasmic free [Ca^{2+}] in midshipman results in the Ca^{2+}-sensitive pumps working closer to their maximum rate. The combination of fast Ca^{2+} pumping and small Ca^{2+} releases permits the midshipman to maintain Ca^{2+} balance in real time during its long-lasting mating call.

MATERIALS AND METHODS

Ethical approval

The animal protocols were approved by the Institutional Animal Care and Use Committees of the University of Pennsylvania and the Marine Biological Laboratory (MBL).

Animals and preparations

Midshipman caught near Bodega Bay, California, were shipped to the MBL, kept at 12°C in seawater tanks, and fed ad libitum. The fish used for the Ca^{2+} transient measurements were subsequently shipped overnight from MBL to the University of Pennsylvania. On the day of an experiment, a fish was sedated in ice-cooled water until unresponsive, then killed by cervical sectioning and double-pithing. The swimbladder was quickly removed and placed in chilled fish Ringer's (composition [mM]: 132 NaCl, 2.6 KCl, 1 $MgCl_2$, 2.7 $CaCl_2$, 10 imidazole, and 10 sodium pyruvate, pH 7.7 at 15°C). Fiber bundles of pure fiber type were dissected out as previously described for toadfish (Rome et al., 1996; Harwood et al., 2011) and checked for twitches by electrical stimulation. Based on the presence of male gonads and the dramatically enlarged reddish swimbladder muscles, most midshipman used in the experiments were type I males, i.e., the type capable of contracting their swimbladder muscle at high frequency for many tens of minutes, thereby producing a continuous call or "hum" to attract gravid females to their nest. For comparison, several skinned fiber experiments were conducted on female midshipman, which are incapable of producing hums.

Skinned fiber experiments

For the ATPase experiments, bundles of ~100 fibers were depolarized in a high potassium solution (composition [mM]: 7.8 $MgCl_2$, 50 K_2EGTA, 1 KH_2PO_4, 6.2 NaATP, and 58.2 TES($C_6H_{15}NO_6S$), pH 7.1 at 15°C). From this, smaller bundles of two to four fibers (fiber diameter ~40 µm) were dissected and chemically skinned with 50 µg/ml saponin for 20 min at 4°C. This permeabilizes the cell membrane but does not affect the Ca^{2+} pumps or SR membrane (Stienen et al., 1995; Launikonis and Stephenson, 1997; Rome et al., 1999b). The fiber bundle was secured between a force transducer (400 series; Aurora Scientific) and a fixed hook with foil clips. Sarcomere length, determined by microscopy (Rome et al., 1990), was set at 3.3 µm (note that type 1 male fibers have very long Z-bands, ~1 µm, and hence have a very long resting sarcomere length; Bass and Marchaterre, 1989).

ATP utilization was measured with a fluorescent-coupled assay (Stienen et al., 1995) in a 5.5-µl temperature-controlled chamber (15 ± 0.1°C) that was vigorously stirred. The Ca^{2+}-EGTA solutions were the same as previously described (Rome and Klimov, 2000). To block SR Ca^{2+} pumping, a cocktail of 20 µM 2,5-di-(tert-butyl)-1,4-benzohydroquinone (TBQ) and 20 µM cyclopiazonic acid (CPA) was used (Rome and Klimov, 2000). Stock solutions of TBQ (7.5 mM), CPA (7.5 mM), and to block cross-bridge activity, *N*-benzyl-*p*-toluene sulfon-

amide (BTS; 20 mM; Cheung et al., 2002) were made in DMSO. We have previously shown that the final concentration of DMSO (≤0.3%, vol/vol) has no effect on ATP utilization by either the cross-bridges or the SR Ca^{2+} pumps (Young et al., 2003). All solutions contained 5 mM caffeine to prevent buildup of Ca^{2+} in the SR and consequent back-inhibition of SR Ca^{2+} pumping. Previous experiments showed that fiber ATP utilization was constant over caffeine concentrations ranging from 2 to 20 mM (Stienen et al., 1995).

In toadfish fibers, 20 µM BTS blocks ATP utilization by the cross-bridges but not by the SR Ca^{2+} pumps (Young et al., 2003); thus, we used a solution with 20 µM BTS in midshipman fibers to measure the relation between $[Ca^{2+}]$ and SR Ca^{2+} pumping. The slope of the curve relating fluorescence intensity and time at a given $[Ca^{2+}]$ was used as a measure of the SR Ca ATPase activity. A stoichiometry of 2 Ca^{2+} per ATP for Ca^{2+} pumping was assumed. At the end of each experiment, the fiber bundle was dried, the clips were removed, and the bundle weight was determined using a microbalance (model C-35; Cahn). The bundle wet weight was calculated using a scaling factor of 8 (Rome and Klimov, 2000). The intact fiber volume was calculated assuming a fiber density of 1.05 kg/l.

Calcium indicator measurements in intact fibers

The Ca^{2+}-indicator methods used in individual midshipman swimbladder fibers were similar to those described previously for furaptra and Fluo-4 in toadfish (Rome et al., 1996; Harwood et al., 2011; Nelson et al., 2014). Experiments on midshipman fibers proved more difficult than those on toadfish fibers, primarily because the midshipman fibers were less hardy than toadfish fibers. Also, the Ca^{2+} transient in midshipman fibers was about an order of magnitude smaller than that in toadfish, which added to the difficulty of resolving the Ca^{2+} transient. For the latter reason, Mag-fluo-4 (Life Technologies) rather than furaptra was used as the primary Ca^{2+} indicator. Mag-fluo-4 has kinetics for Ca^{2+} and Mg^{2+} binding that are similar to those of furaptra but gives an ~12-times-larger fluorescence signal.

A small bundle of swimbladder fibers was isolated by dissection and mounted on an optical bench apparatus in an experimental chamber containing fish Ringer's (16°C). The apparatus was equipped to measure resting fluorescence and changes in fluorescence during activity from a short length, ~300 µm, of the fiber bundle. The main results were obtained on eight fibers from four fish in which the potassium-salt form of the indicator (K_4Mag-fluo-4) was introduced into the myoplasm of one fiber on the surface of a fiber bundle by pressure injection. Supportive information was obtained on one other fiber from one other fish in which Fluo-4 (a high-affinity, Ca^{2+}-specific indicator) was used instead of Mag-fluo-4 (see last section of Results). Fluorescence was measured 10–100 min after indicator injection from a region of the bundle centered 0.3 to 1 mm from the injection site; the bandpass of the fluorescence excitation and emission filters was 450–490 nm and ≥510 nm, respectively. The mean concentration of Mag-fluo-4 at the measurement site was estimated to be 74 ± 14 µM (n = 8; see also legend of Table 1).

Table 1. **Concentrations of the myoplasmic constituents in the midshipman swimbladder model**

Constituent	Concentration	Concentration of binding sites
	µM	*µM*
Resting free $[Ca^{2+}]$	0.030	-
Resting free $[Mg^{2+}]$	1,000	-
Troponin	73	73 (Ca^{2+} regulatory sites)
Parv	520	1040 (Ca^{2+}/Mg^{2+} sites)
SR Ca^{2+} pump	980	1,960 (Ca^{2+} transport sites)
ATP	8,000	8,000 (Ca^{2+}/Mg^{2+} sites)
Mag-fluo-4	50–100	50–100 (Ca^{2+} sites)

All concentrations are spatially averaged and referenced to the myoplasmic water volume in the myofibrillar region, except for free $[Ca^{2+}]$ and free $[Mg^{2+}]$, for which total concentrations are given. The concentrations are taken from Nelson et al. (2014); those for troponin and Parv have been adjusted for measured anatomical, biochemical, and physiological differences between midshipman and toadfish swimbladder fibers (see Materials and methods). The concentration of Mag-fluo-4 was estimated from a comparison of the resting fluorescence of Mag-fluo-4 in midshipman fibers with that in frog twitch fibers, with an appropriate scaling for the measured differences in fiber diameters; the 100-µM value applies to measurements made early in an experiment (as in Figs. 1 and 3 and Table 2), whereas the 50-µM value applies to measurements made later in an experiment (cf. Figs. 4, 5, and 6).

Changes in indicator fluorescence (ΔF) were elicited by a propagating AP or a train of APs set up by pointwise stimulation from a pair of extracellular electrodes located near the bundle surface close to the injection site; only fibers that responded with all-or-nothing ΔF signals were studied. From the time of onset of ΔF at different distances from the point of stimulation, the conduction velocity of the AP at 16°C was estimated to be 0.80 ± 0.01 mm/ms (n = 3). This relatively slow velocity is similar to that observed in toadfish swimbladder fibers, 0.61 + 0.11 mm/ms (n = 5). This similarity is consistent with the possibility that midshipman swimbladder fibers are multiply innervated, as occurs in toadfish.

In most experiments, 5–10 µM BTS was included in the Ringer's solution to reduce movement artifacts in the ΔF records. This concentration appeared to be less effective in reducing movement than was observed previously in toadfish fibers, but to avoid possible pharmacological broadening of the AP, larger concentrations were not used (Cheung et al., 2002). To further reduce movement, the bundles were stretched to a mean sarcomere length of 3.9 ± 0.2 µm (n = 4; range 3.4–4.4 µm), which is somewhat longer than that found in situ in type I males, 3.3 µm (see Skinned fiber experiments).

For analysis, the ΔF signals were normalized by the indicator's resting fluorescence, F_R, which was obtained in a two-step procedure. First, the estimated contribution of the bundle's intrinsic fluorescence, F_{Int}, was

subtracted from the raw value of the bundle's resting fluorescence at the measurement site to yield the indicator-related resting fluorescence, F_{Dye}. F_{Int} was measured from a bundle region that did not contain indicator, located 1–2 mm along the fiber bundle from the measurement site. Second, F_{Dye} was multiplied by 0.568 to yield F_R, the value used to normalize ΔF. This scaling was applied because F_{Dye} arises from indicator located in the cytoplasm of three anatomically distinct regions of the injected fiber: (a) the periphery, which is densely packed with mitochondria but lacks myofibrils; (b) the central core, which also has a substantial density of mitochondria and lacks myofibrils; and (c) the myofibrillar region, which is an annulus-shaped region between the periphery and the central core that contains the contractile filaments but is almost devoid of mitochondria (Bass and Marchaterre, 1989; Brantley et al., 1993). The myofibrillar region also contains a well-developed network of SR membranes with triadic junctions, the sites of SR Ca^{2+} release. The fraction of the cytoplasmic water volume in the myofibrillar region is estimated to be 0.568, which therefore gives the fraction of F_{Dye} that arises from the myofibrillar region. (The corresponding fraction estimated for toadfish swimbladder fibers is 0.685 [Harwood et al., 2011].) As in toadfish fibers, F_R, rather than F_{Dye}, was used to normalize ΔF because (a) ΔF is thought to arise primarily from the myofibrillar region and (b) the goal of the simulations described in Model simulations was to estimate the Ca^{2+}-related changes in the myofibrillar region.

In most experiments, the estimate of F_{Dye}, and hence of F_R, had some uncertainty. This occurred because F_{Dye} was relatively small, only 1.06 ± 0.19 times F_{Int} (range 0.41–1.74; $n = 8$). F_{Dye} was small because (a) the amount of indicator injected into a fiber was kept small to avoid indicator concentrations that would have a substantial buffering effect on the stimulated change in the myoplasmic free Ca^{2+} concentration ($\Delta[Ca^{2+}]$); (b) the fluorescence of Mag-fluo-4 in a resting fiber is relatively low because most of the indicator is in its metal-free (low-fluorescence) form at rest; and (c) the mean diameter of the injected fibers was small, 33 ± 1 µm (n = 6; range 31–37 µm). Although the estimate of F_{Dye} had some uncertainty, the peak amplitude of $\Delta[Ca^{2+}]$ elicited by an AP, which was calculated from Mag-fluo-4's $\Delta F/F_R$ (next section), was found to be similar in the eight experiments (Table 2; described in Results). This similarity indicates that the method for estimation of F_{Dye} is likely to have been reasonably accurate.

Estimation of $\Delta[Ca^{2+}]$ from $\Delta F/F_R$

Mag-fluo-4's $\Delta F/F_R$ was first converted to an equivalent furaptra signal based on the relationship between the Mag-fluo-4 and furaptra $\Delta F/F_R$ signals determined previously in frog twitch fibers (Hollingworth et al., 2009). When injected simultaneously into a frog fiber, the two signals have the same time course, but the amplitude of the furaptra signal (410 ± 20-nm excitation, 470–590-nm emission) is smaller than that of the Mag-fluo-4 signal (450–490-nm excitation, ≥510-nm emission) by a factor of −1/12. The equivalent furaptra signal, obtained by scaling the Mag-fluo-4 signal by the factor −1/12, was then calibrated in terms of $\Delta[Ca^{2+}]$ with our method for calibrating the furaptra $\Delta[Ca^{2+}]$ signal in frog. This approach permitted a direct comparison of the midshipman $\Delta[Ca^{2+}]$ signal with that measured previously in toadfish with furaptra (Rome et al., 1996; Harwood et al., 2011). The calibration used the equations described previously for furaptra (Baylor and Hollingworth, 2003):

$$\Delta f_{CaD} = -1.07 \times (\Delta F/F_R), \quad (1)$$

$$\Delta[Ca^{2+}] = K_{D,Ca} \times \Delta f_{CaD}/(1 - \Delta f_{CaD}), \quad (2)$$

where Δf_{CaD} denotes the fraction of the indicator that switches from the Ca^{2+}-free to the Ca^{2+}-bound form during activity, and $K_{D,Ca}$ denotes the apparent dissociation constant of furaptra in the myoplasm when the fiber is stimulated by an action-potential and was assumed to be 96 µM (Konishi et al., 1991; Baylor and Hollingworth, 2003). The use of Eq. 2 assumes that furaptra tracks $\Delta[Ca^{2+}]$ with a negligible kinetic delay (Konishi et al., 1991) and that a negligible fraction of the indicator is in the Ca^{2+}-bound form at rest (Konishi et al., 1993). The value of Δf_{CaD} calculated with Eq. 1 was assumed to apply to Mag-fluo-4 because the value of $K_{D,Ca}$ for Mag-fluo-4 measured in this study (52 ± 6 µM; mean ± SEM; n = 4) in 130 mM KCl and the absence of Mg^{2+} (20°C–21°C, pH 7.0) is similar to that measured for furaptra (44 µM; Konishi et al., 1991). The Mg^{2+} dissociation constant of Mag-fluo-4 ($K_{D,Mg}$), measured at pH 7.0 and 21°C in the absence of Ca^{2+}, is 6.5 mM (Hollingworth et al., 2009).

Model calculations

The major movements of Ca^{2+} in the fiber's myofibrillar region during activity were estimated from $\Delta[Ca^{2+}]$ with a single-compartment (spatially averaged) kinetic model, similar to that used for toadfish swimbladder fibers (Rome et al., 1996; Harwood et al., 2011; Nelson et al., 2014). Although the Ca^{2+} movements estimated with a single-compartment model are only approximate, the results in midshipman fibers can be compared with similarly estimated movements in toadfish fibers. As previously, the model calculations were performed with MLAB (Civilized Software), a high-level mathematical modeling language.

Table 1 gives the concentrations of the myoplasmic constituents included in the model; these are referenced to the myoplasmic water volume in the myofibril-

lar region of the fiber (Baylor et al., 1983; Harwood et al., 2011). These concentrations, as well as the schemes and rate constants for the reactions of Ca^{2+} (and, in some cases, Mg^{2+}) with the divalent-ion binding species, are based on those in the toadfish model (Harwood et al., 2011; Nelson et al., 2014). The changes made for the midshipman modeling are as follows (see also Results).

(1) The concentration of Parv is 520 µM (vs. 2,670 µM in toadfish). This value takes into account (a) the eightfold smaller concentration of Parv per wet weight of muscle in superfast fibers of midshipman compared with toadfish (Tikunov and Rome, 2009) and (b) an adjustment for the smaller myoplasmic volume estimated for midshipman fibers compared with toadfish fibers.

(2) The concentration of troponin is 73 µM (vs. 106 µM in toadfish). This value takes into account the dilution of the troponin concentration in the myofibrillar region of the fiber because of the presence of the unusually wide Z-bands in Type I midshipman males (see Skinned fibers experiments).

(3) Troponin is assumed to have one Ca^{2+} regulatory site per molecule (vs. two in toadfish) and a Ca^{2+} dissociation constant of 5.2 µM (vs. 3.9 µM in toadfish). The selection of these values reflects the finding that the tension–pCa curve in midshipman fibers is less steep than that in toadfish fibers (see Results). With an on-rate constant of 0.885×10^8/M/s for the reaction of Ca^{2+} with the troponin regulatory sites (as assumed in toadfish fibers), the calculated off-rate constant for the Ca^{2+}–troponin reaction in midshipman is 460/s (vs. 345/s for each troponin site in toadfish).

Given $\Delta[Ca^{2+}]$ calculated with Eq. 2, the differential equations that define the kinetic responses of the model constituents can be solved simultaneously to estimate the total concentration of Ca^{2+} released by the SR (denoted $\Delta[Ca_T]$) and the rate at which Ca^{2+} is released (denoted R_{REL}, calculated as $(d/dt)\Delta[Ca_T]$). $\Delta[Ca_T]$ is obtained as the sum of seven changes: $\Delta[Ca^{2+}]$ itself; the changes in the concentration of Ca^{2+} bound to the Ca^{2+} regulatory sites on troponin (Δ[CaTrop]) and to the metal sites on ATP (Δ[CaATP]), Parv (Δ[CaParv]), the SR Ca^{2+} pump (Δ[CaPump]), and the indicator dye (Δ[CaDye]); and the change in concentration of Ca^{2+} pumped by the SR Ca^{2+} pumps (Δ[CaPumped]).

Model simulations

As described in the preceding section, given a measured $\Delta[Ca^{2+}]$ waveform, the computational model can be used to obtain estimates of (a) the concentration changes of Ca^{2+} bound to the various myoplasmic Ca^{2+}-binding sites, (b) the change in the concentration of Ca^{2+} pumped by the SR Ca^{2+} pumps, and (c) the amount and time course of SR Ca^{2+} release (R_{REL}). The same system parameters can also be used in an alternate modeling mode in which an assumed waveform of R_{REL} is used as input to the model, with the output being (a) $\Delta[Ca^{2+}]$, (b) the concentration changes of Ca^{2+} bound to the various myoplasmic Ca^{2+} binding sites, and (c) the change in the concentration of Ca^{2+} pumped by the SR Ca^{2+} pumps. In this mode, the amplitude of R_{REL} is adjusted so that the amplitude of the simulated $\Delta[Ca^{2+}]$ waveform approximately matches that of the measured $\Delta[Ca^{2+}]$ waveform. These calculations, which are noise-free and referred to as "simulations," were performed to help interpret the indicator measurements recorded from fibers that were stimulated repetitively for many seconds. In such experiments, the measured $\Delta[Ca^{2+}]$ signal (Eqs. 1 and 2) was small and noisy, so the modeling mode described in the preceding section was less useful because its output waveforms were very noisy.

For the simulations, the SR Ca^{2+} release waveform elicited during each cycle of a long stimulus train was assumed to satisfy the following function (Nelson et al., 2014):

$$\begin{aligned} R_{REL}(t) &= 0 \text{ if } t < T; \\ &= R \cdot \{1 - \exp[-(t-T)/\tau 1]\}^5 \cdot \exp[-(t-T)/\tau 2] \text{ if } t \geq T. \end{aligned} \quad (3)$$

R is the factor that sets the amplitude of the release waveform, and T is the time of the stimulus. For all releases, the values of $\tau 1$ and $\tau 2$ were set to 0.8 and 0.32 ms, respectively, so that the full duration at half-maximum (FDHM) of each release waveform would be 1.0 ms (the value estimated in connection with Fig. 3, described in Results). To relate the simulations to the $\Delta[Ca^{2+}]$ signal measured during a long stimulus train, R for each shock was chosen so that the peak of each $\Delta[Ca^{2+}]$ in the simulated $\Delta[Ca^{2+}]$ waveform approximately matched the corresponding peak in the measured waveform. As described in Results (Fig. 5 and related text), when a fiber is stimulated at a constant frequency for many seconds, a steady state is reached in which the measured $\Delta[Ca^{2+}]$ signal elicited by each shock in the train is approximately the same. Therefore, for the simulations described in Fig. 6 (see Results), an appropriate value of R was selected for use in Eq. 3; this one value was then applied to every cycle in the long stimulus train until a steady state was reached.

Statistical analysis

The principal data are reported as means ± SEM. *t* tests at $P < 0.05$ were used to test for statistical significance.

RESULTS

The force and $\Delta[Ca^{2+}]$ responses elicited by an AP

As noted in Materials and methods, living midshipman fibers proved to be a challenging experimental preparation on which to work. In the experimental results described in Figs. 1, 3, 4, 5, 6, and 7, the highest-frequency electrical stimulation that the fibers appeared capable of following fell in the range 67–100 Hz. For the

recordings shown in the figures, the highest response frequency sustainable by that preparation was usually selected. Fig. 1 A shows two examples of the twitch response measured at 15°C from a bundle of midshipman swimbladder fibers that was stimulated by a brief shock at zero time. The peak value and the FDHM of the twitch are 2.1 kN/m^2 and 9.2 ms for the lower trace and 1.8 kN/m^2 and 10.6 ms for the upper trace. These values are close to the mean values observed in five experiments of this type on five fish, 1.6 ± 0.2 kN/m^2 and 10.9 ± 0.2 ms (Table 2).

Fig. 1 (C and E) shows examples from two experiments of Ca^{2+}-related signals measured during a twitch at 16°C. In each panel, the lower trace shows the Mag-fluo-4 $\Delta F/F_R$ signal recorded from the injected fiber on the surface of the fiber bundle. The early change in fluorescence (time of peak ~4 ms) monitors the Ca^{2+} transient that arises within the myofibrillar region of the fiber in response to the AP. The peak amplitude and FDHM of $\Delta F/F_R$ are 0.62 and 2.0 ms in Fig. 1 C and 0.77 and 1.9 ms in Fig. 1 E. These values are close to the mean values observed in eight similar experiments on four fish, 0.64 ± 0.04 and 1.9 ± 0.1 ms, respectively.

In Fig. 1 C, the $\Delta F/F_R$ signal appears to be essentially free of a movement artifact, as the signal returns smoothly toward baseline during the time of the ex-

Table 2. **Properties of the force and Δ[Ca^{2+}] response in midshipman swimbladder fibers stimulated by an AP (15–16°C)**

Property	Force (15°C)	Δ[Ca^{2+}] (16°C)
10–100% rise time (ms)	6.1 ± 0.3 (5)	0.9 ± 0.0 (8)
FDHM (ms)	10.9 ± 0.2 (5)	1.9 ± 0.1 (8)
Peak amplitude	1.6 ± 0.2 kN/m^2 (5)	5.7 ± 0.4 μM (8)

The entries are mean ± SEM values (number of experiments). In the second column, peak amplitude has been referenced to the cross-sectional area of the bundle; in the third column, Δ[Ca^{2+}] was estimated from the Mag-fluo-4 $\Delta F/F_R$ referenced to the myofibrillar region of the fiber (see Materials and methods). Of the eight fibers that contributed to the data in the third column, four appeared to have Δ[Ca^{2+}] signals whose falling phase was free of a movement artifact, and four appeared to have a small negative-going movement artifact at 7–12 ms (as in Fig. 1 E). A slightly briefer value of FDHM was observed for the latter fibers compared with the former, 1.8 ± 0.1 vs. 2.0 ± 0.1 ms; this indicates that the movement artifact may have artifactually reduced the estimate of FDHM by a small amount.

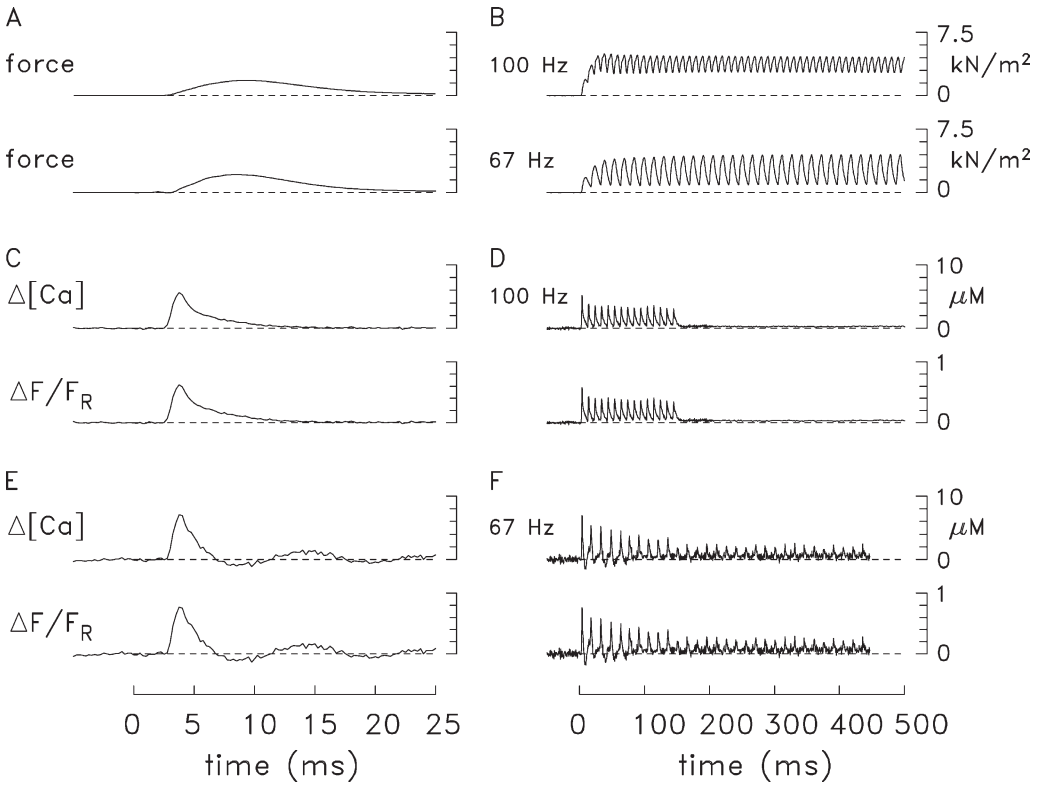

Figure 1. **Examples of force responses and myoplasmic calcium transients from midshipman swimbladder fibers stimulated by APs.** The labels on the far left and far right apply to both sides of the figure. **(A)** Examples of the twitch response from two different bundles of midshipman fibers excited by a one-shock field stimulus at zero time. **(B)** Force responses from the bundle corresponding to the upper trace in A in response to 67- and 100-Hz stimulation. **(C)** Mag-fluo-4 $\Delta F/F_R$ and Δ[Ca^{2+}] signals during a twitch from one fiber on the surface of a swimbladder bundle; the signals were elicited by a pointwise (not field) stimulation. **(D)** $\Delta F/F_R$ and Δ[Ca^{2+}] signals from the same fiber as in C when stimulated by 15 shocks at 100 Hz. **(E and F)** Responses like those in C and D from a different fiber and bundle; in F, the stimulus was 30 shocks at 67 Hz. The records in E and F reveal a slight a movement artifact. Experiment no. 051413.1 (C and D), 052114.1 (E and F).

pected force response (compare Fig. 1 A). A similar smooth return was seen in four of the eight experiments. In contrast, in Fig. 1 E, the $\Delta F/F_R$ trace has an oscillatory movement artifact that likely became significant later in the falling phase of the early signal. The presence of this artifact masks the true time course with which the Ca^{2+}-related component of the signal returns toward baseline. A similar oscillatory movement artifact of this type was seen in the other four of the eight experiments.

In Fig. 1 (C and E), the upper trace shows $\Delta[Ca^{2+}]$ estimated by means of Eqs. 1 and 2 from the corresponding $\Delta F/F_R$ signal. The values of peak amplitude and FDHM are 5.4 µM and 2.0 ms in Fig. 1 C and 7.0 µM and 1.9 ms in Fig. 1 E. These values are close to the mean values observed in the eight experiments of this type: 5.7 ± 0.4 µM and 1.9 ± 0.1 ms, respectively (Table 2).

Force and $\Delta[Ca^{2+}]$ responses elicited by a high-frequency train of APs

Fig. 1 B shows force responses from one of the bundles of Fig. 1 A when it was stimulated at 67 and 100 Hz. During the time of stimulation, both traces show a well-maintained oscillation in force, which underlies the ability of the swimbladder to generate sound under in vivo conditions. This oscillation reached an approximate steady state after a brief buildup of baseline force; this buildup occurred because the stimulation frequency was too fast for the bundle to fully relax after each shock in the train.

Fig. 1 (D and F) shows examples of Ca^{2+}-related signals measured during high-frequency stimulation of the fibers of Fig. 1 (C and E), respectively. In Fig. 1 D, the fiber was stimulated by a 100-Hz stimulus that lasted 0.15 s (total of 15 shocks). The $\Delta[Ca^{2+}]$ trace reveals a well-resolved change with each shock that appears to be free of a movement artifact (as in Fig. 1 C) and returns almost to baseline between shocks. The peaks in the $\Delta[Ca^{2+}]$ waveform caused by the later shocks are ~3.5 µM, which is somewhat smaller than that caused by the first shock, ~5 µM. After cessation of stimulation, the $\Delta[Ca^{2+}]$ trace declined quickly to a quasi-steady level that remained slightly above baseline during the remainder of the sweep. By the end of the recording (350 ms after cessation of stimulation), the elevation in baseline $[Ca^{2+}]$ (calculated with Eqs. 1 and 2) is 0.30 µM. This value is likely to be an overestimate because Mag-fluo-4 has some sensitivity to Mg^{2+} (see Materials and methods), and myoplasmic free $[Mg^{2+}]$ likely also increases with activity because of an exchange of Ca^{2+} for Mg^{2+} on Parv (e.g., Harwood et al., 2011).

In Fig. 1 F, the recording period lasted 0.5 s, during which the fiber was stimulated by a 67-Hz stimulus for 0.45 s (total of 30 shocks). As expected from Fig. 1 E, the traces reveal a movement artifact at early times after onset of stimulation; the artifact, however, appears to become insignificant after the first five or six shocks in the train. In contrast with Fig. 1 D, the peaks in the $\Delta[Ca^{2+}]$ waveform in Fig. 1 F reveal a somewhat greater fractional decline during the first 15 responses, after which an approximate steady state is reached; the mean peak of $\Delta[Ca^{2+}]$ during the last 20 responses is ~2.0 µM. The estimated elevation in baseline $[Ca^{2+}]$ during the last 20 responses, as determined from the mean value of the low points in the $\Delta[Ca^{2+}]$ waveform, is 0.46 µM. As mentioned, this is likely to be an overestimate because of a concurrent increase in $[Mg^{2+}]$.

The SR Ca^{2+} pumping–pCa relationship measured in skinned fibers

We found that the relationship between normalized ATP utilization by SR Ca^{2+} pumping and $[Ca^{2+}]$ in type I male midshipman swimbladder fibers (Fig. 2 A, black) was similar to that in male toadfish swimbladder (Young et al., 2003). The pCa_{50} was 6.13 ± 0.06 (n = 8) compared with 6.08 ± 0.156 (n = 9) for toadfish. The Hill coefficient was higher in the midshipman fibers (1.76 ± 0.121) compared with toadfish (1.49 ± 0.04), but this difference is not large. A bigger difference, however, was noted in the maximum rate of SR Ca^{2+}pump ATP utilization, which was 0.69 ± 0.125 mmol/s/kg in midshipman compared with 1.0 in toadfish. Because 2 Ca^{2+} are pumped per ATP consumed, this corresponds to 1.4 mmol/s/kg in midshipman compared with 2 mmol/s/kg in toadfish.

We observed a significant difference between female and type 1 male midshipman swimbladder muscle. The female muscle had a higher SR Ca^{2+} pump ATP utilization rate (1.07 ± 0.083 mmol/s/kg; n = 10, which is very similar to that in male toadfish) and a correspondingly higher Ca^{2+} pumping rate (2.14 mmol/s/kg). The likely explanation of the lower SR Ca^{2+}ATP utilization in the type 1 male midshipman has to do with the amount of space in the muscle cell devoted to SR. The muscles of females are quite white in color compared with the deep red of the type 1 male swimbladder. The latter is a manifestation of the high aerobic capacity and hence a large volume of mitochondria in the type 1 male midshipman swimbladder muscle, which is necessary to generate the ATP required for high-frequency contractions for long periods of time. In contrast, females do not produce high-frequency hums. They produce only an occasional short grunt and accordingly have a very low mitochondrial density (Bass and Marchaterre, 1989). Similarly, male toadfish have a low-duty-cycle call (~5%) and hence they do not need real-time ATP production as high as that of type 1 male midshipman; accordingly their mitochondrial volume is only ~4% of fiber volume (Appelt et al., 1991) compared

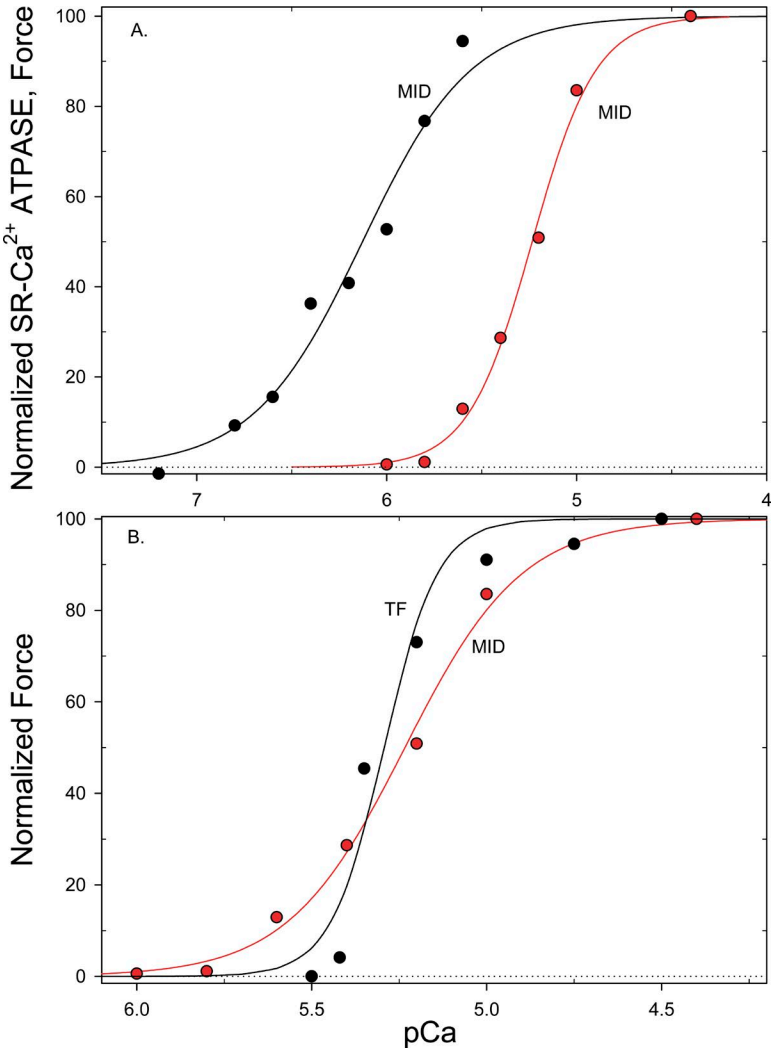

Figure 2. **SR Ca^{2+} pump ATPase versus pCa and force versus pCa in swimbladder fibers. (A)** Representative experiments showing normalized SR Ca^{2+} ATP utilization (black) and force (red) as a function of pCa. For the SR Ca^{2+} ATP utilization measurement, the fiber was treated in BTS, so that nearly all of the measured ATP utilization was associated with SR Ca^{2+} pumping. At higher $[Ca^{2+}]$ than pCa = 5.6, the ATP utilization declined (not depicted), hence the Hill equation was fitted to data up to pCa = 5.6 in this preparation. The pCa_{50} was 6.13 and the Hill coefficient was 1.52. Note that we also previously observed an SR Ca^{2+} ATP utilization decline at high $[Ca^{2+}]$ in toadfish (Young et al., 2003). Data for the force–pCa relation (which were measured on another preparation) were also fitted with the Hill equation. Force was much less sensitive to $[Ca^{2+}]$ than was Ca^{2+} pumping. The pCa_{50} was 5.23 and the Hill coefficient was 2.58. Because of the right-shifted force–pCa relation, at certain $[Ca^{2+}]$ values (e.g., pCa = 6), the fiber can pump Ca^{2+} at a relatively high rate but not generate force. Both plots are labeled MID for midshipman. **(B)** Representative force–pCa curves from toadfish and male midshipman muscle fibers. Shown is the same midshipman fiber (red, MID) as illustrated in A. The toadfish fiber (black, TF) is from Rome et al. (1996). Note that the toadfish fiber has a much steeper force–pCa relationship than the midshipman fiber, and for a 0.2 change in pCa units, toadfish force jumps by 66% compared with 43% for midshipman.

with ~40% in midshipman (estimated from Bass and Marchaterre [1989], Brantley et al. [1993], and Lewis et al. [2003]).

As pointed out by Rome and Lindstedt (1998), space in a muscle cell represents a zero sum game among three main components: force-generating myofibrils, mitochondria, and SR. In type 1 males of midshipman, the 40% of the fiber volume devoted to the mitochondria reduces space available for the SR and myofibrils. Not only is the fractional cross section of the SR reduced, but a further reduction in SR volume arises because of the long 1-µm Z-bands in type 1 male midshipman (Bass and Marchaterre, 1989) compared with the 0.05-µm value in toadfish. In type 1 male fibers, the resting sarcomere length is ~3.3 µm, of which only ~2.2 µm contains the thick and thin filaments, where SR is concentrated. Hence the elongated Z-bands further reduce SR volume.

The normalized relation of the SR Ca pump ATP utilization versus pCa in female midshipman (not depicted) is quite similar to that found for toadfish and is not very different from that of the type 1 male midshipman. The pCa_{50} is 6.02 ± 0.053, and the Hill coefficient is 1.40 ± 0.04.

Force–pCa relationship

The normalized muscle force–pCa curve of the type 1 male midshipman swimbladder (Fig. 2, red) is visually less steep (Fig. 2 B) than that of the toadfish (Rome et al., 1996). When fitted with the Hill equation, however, the difference in the resulting Hill coefficients was more equivocal. This apparent discrepancy is because of the toadfish swimbladder force–pCa data not being well fitted by the Hill equation, as first observed in Rome et al. (1996). We therefore used another approach for comparison, which did not require curve fitting. We compared the maximum change in force measured for a given change in pCa. We found that the type 1 male midshipman force–pCa is significantly less steep than that of the toadfish. In toadfish, the maximum change in force was 55.22 ± 1.87% (n = 4) for 0.1 change in pCa and 63.32 ± 2.05% (n = 4) for a 0.2 change in pCa. Midshipman force was only measured every 0.2 pCa units, and the maximum change was 41.82 ± 3.16% (n = 5).

Comparison of SR Ca^{2+} pumping and force generation as a function of Ca^{2+} concentration

Fig. 2 A shows typical midshipman results for the dependence of SR Ca^{2+} pumping and force as a function of pCa. The force generation curve (pCa_{50} = 5.23) is strongly right-shifted compared with Ca^{2+} pumping (pCa_{50} = 6.13); this allows a fiber to pump Ca^{2+} at a relatively high rate in the absence of force production.

Model estimates of myoplasmic Ca^{2+} movements during a twitch

The initial model used to estimate myoplasmic Ca^{2+} movements in active midshipman fibers followed that used previously in toadfish fibers (Harwood et al., 2011; Nelson et al., 2014). The parameters of the model were unchanged except for the number of Ca^{2+} regulatory sites on each troponin molecule (one in midshipman vs. two in toadfish) and the concentrations of Parv and troponin (see Materials and methods). This approach allowed a reasonably direct comparison to be made between results in midshipman and toadfish fibers. Two additional modifications to the midshipman modeling were also explored: (1) a change in the number of Ca^{2+} regulatory sites on each troponin molecule from one to two (compare Fig. 4 B) and (2) an increase in the sensitivity of the Ca^{2+} pumping-versus-pCa relation (compare the penultimate section of Results, Simulations with a more-sensitive Ca^{2+} pumping–pCa relation). This latter change was made so that the sensitivity of Ca^{2+} pumping approximately matched that in midshipman measurements on skinned fibers. As noted in the penultimate section of the Results, both of these changes had relatively minor effects on the quantitative conclusions and no effect on the qualitative conclusions.

Fig. 3 shows estimated Ca^{2+} movements in the myofibrillar region of a midshipman fiber when the measured $\Delta[Ca^{2+}]$ trace of Fig. 1 C was used as the input to the model; the properties of this $\Delta[Ca^{2+}]$ trace are close to the mean experimental properties during a single twitch (compare Table 2). The lowermost trace shows the change in the concentration of Ca^{2+} bound to ATP; the peak of this trace, 20 µM, is 3.7-fold larger than that of $\Delta[Ca^{2+}]$, whereas its time course is essentially identical to that of $\Delta[Ca^{2+}]$. The next trace shows the change in concentration of Ca^{2+} bound to the troponin regulatory sites. As expected physiologically, the FDHM of this trace, 6.4 ms, is briefer than the mean value of FDHM of the twitch response, 10.9 ± 0.2 ms (Table 2). The peak of Δ[CaTrop], 26 µM, corresponds to occupancy of 35% of the troponin regulatory sites with Ca^{2+}. The next two traces show the changes in concentration of Ca^{2+} bound to the metal sites on Parv and to the SR Ca^{2+} pump. Both traces have similar time courses; their peak values correspond to Ca^{2+} occupying 9.0% and 1.7% of these sites, respectively. The two superimposed traces just below the topmost trace show

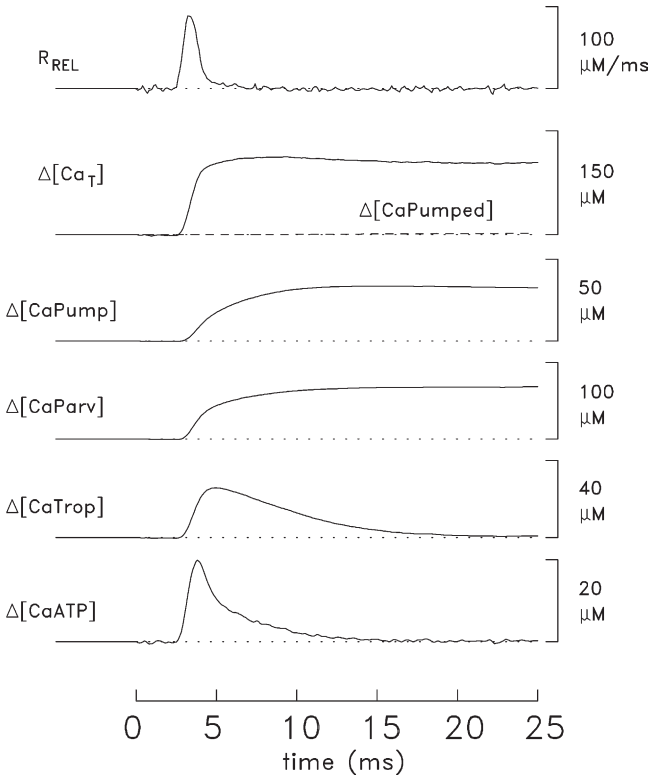

Figure 3. **Model estimates of myoplasmic Ca^{2+} movements during a twitch.** The trace in Fig. 1 C was used as input to the model described in Materials and methods to calculate changes in Ca^{2+} release, binding, and pumping. R_{REL} shows the estimated rate at which Ca^{2+} is released from the SR. The concentration of Ca^{2+} returned to the SR by pumping (dashed trace, labeled Δ[CaPumped]) is almost zero on a time scale of 25 ms.

(a) the total concentration of Ca^{2+} released from the SR (continuous trace, labeled $\Delta[Ca_T]$), whose peak value is 113 µM, and (b) the concentration of Ca^{2+} that has been returned to the SR by Ca^{2+} pumping (dashed trace, labeled Δ[CaPumped]), which barely rises above the dotted baseline and whose value is ∼2.2 µM at 25 ms. The uppermost trace, R_{REL} (calculated by (d/dt) $\Delta[Ca_T]$), shows the estimated rate of SR Ca^{2+} release; the peak value and FDHM are 89 µM/ms and 1.1 ms, respectively. This peak is eightfold smaller than that estimated for the myofibrillar region of a toadfish swimbladder fiber during a twitch, 700 µM/ms, whereas the FDHM is similar to that for toadfish, 1 ms (Harwood et al., 2011; Nelson et al., 2014). The small peak of R_{REL} in midshipman fibers, which is a major finding of this study, represents an important functional difference between swimbladder fibers of midshipman and toadfish.

If the $\Delta[Ca^{2+}]$ trace in Fig. 1 C is free of a movement artifact and if the model accounts for all significant myoplasmic Ca^{2+} movements, the $\Delta[Ca_T]$ trace in Fig. 3 is expected to rise to an early peak and remain constant thereafter. Although this expectation holds approximately, the $\Delta[Ca_T]$ trace decays slightly between 8 and

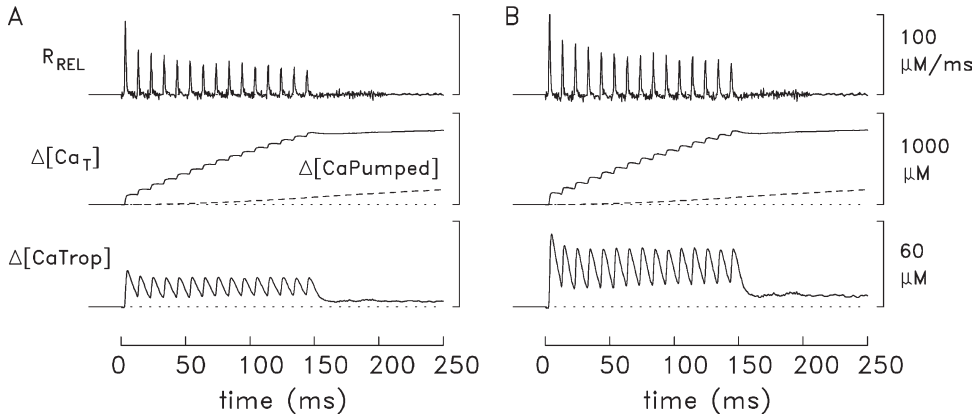

Figure 4. **Model estimates of myoplasmic Ca^{2+} movements during a brief high-frequency stimulus. (A)** Selected estimates like those in Fig. 3 except that the $\Delta[Ca^{2+}]$ trace in Fig. 1 D was used as input to the model. **(B)** As in A except that the number of Ca^{2+}-regulatory sites per troponin molecule was assumed to be two rather than one (see text). All labels apply to the corresponding traces on both sides of the figure.

25 ms, and correspondingly, the R_{REL} trace of Fig. 3 slightly undershoots the baseline between 8 and 25 ms. This feature of the calculations indicates that the estimate of $\Delta[Ca_T]$ has some error. This could arise because of one or more of the following reasons: (a) the presence of a small movement artifact in the $\Delta[Ca^{2+}]$ trace in Fig. 1 C, (b) a modeling simplification (e.g., associated with the inability of a single-compartment model to account for delays caused by diffusion), or (c) an error in the model (e.g., because of incorrect selection of one or more of the system parameters or omission of a relevant myoplasmic Ca^{2+}-binding species). Nevertheless, the estimates in Fig. 3, including $\Delta[Ca_T]$, appear to be reasonable given the approximate nature of the model.

Model estimates of myoplasmic Ca^{2+} movements during a brief high-frequency stimulus

Fig. 4 A shows additional model calculations, this time with the $\Delta[Ca^{2+}]$ trace of Fig. 1 D used as the input. The Δ[CaTrop] trace associated with the 100-Hz stimulus reveals a maintained oscillation whose peaks and troughs are ∼20 and 7 μM, respectively. The amplitude of the troughs as a fraction of the peaks is smaller than that observed for the 100-Hz force trace in Fig. 1 B, consistent with the expectation that the kinetics of troponin activation and deactivation should be faster than the kinetics of force development and relaxation. The $\Delta[Ca_T]$ trace in Fig. 4 A reveals that (a) the total concentration of Ca^{2+} released by the 15 stimuli is ∼810 μM, and (b) the amount of Ca^{2+} released per stimulus by the last 14 stimuli, the mean of which is ∼50 μM, is only 30–60% of that elicited by the first stimulus, 112 μM. Correspondingly, the peaks of the R_{REL} trace in response to stimuli 2–14 are 30–60% of the first peak (91 μM/ms). As in toadfish fibers (Harwood et al., 2011), the reduced amount of Ca^{2+} release elicited by stimuli after the first is likely a result of the process of Ca^{2+} inactivation of Ca^{2+} release. Also, as in toadfish, some recovery of the release process from inactivation likely takes place between stimuli, because $\Delta[Ca^{2+}]$ returns nearly to baseline between stimuli (Fig. 1 D).

Fig. 4 B shows calculations like those in Fig. 4 A, except that each troponin molecule is assumed to have two Ca^{2+} regulatory sites rather than one. As expected, the Δ[CaTrop] trace in Fig. 4 B reveals a steady oscillation whose peaks and troughs, ∼41 and ∼15 μM, are twice those in Fig. 4 A. The estimate of the total concentration of Ca^{2+} released by the 15 stimuli is only 815 μM, which is barely larger than the 810 μM value in Fig. 4 A, even though the peaks in the R_{REL} trace in Fig. 4 B are, on average, ∼25% larger than the corresponding peaks in Fig. 4 A. This situation arises because, in Fig. 4 B, the decline in the $\Delta[Ca_T]$ trace during each intershock interval is steeper than that in Fig. 4 A; equivalently, the R_{REL} trace in Fig. 4 B has a noticeable baseline undershoot between its peaks. In a well-behaved model, R_{REL} is not expected to undershoot the baseline, so the results in Fig. 4 B reveal a significant shortcoming in this version of the model, which is therefore less satisfactory than that in Fig. 4 A. The results in Fig. 4 thus favor the idea that each troponin molecule has one Ca^{2+} regulatory site rather than two. This conclusion is consistent with the steady-state measurements in Fig. 2 A, in which the tension–pCa curve in midshipman fibers is less steep than that observed previously in toadfish fibers (see Force–pCa relationship). The modeling calculations in the remainder of the paper have been performed under the assumption that each troponin molecule has one Ca^{2+} regulatory site.

Force and $\Delta[Ca^{2+}]$ responses during long-lasting high-frequency stimulation

In Fig. 5, the upper traces show force responses from a fiber bundle that was stimulated continuously at 83 Hz for 5 s. The response at the start of stimulation is shown

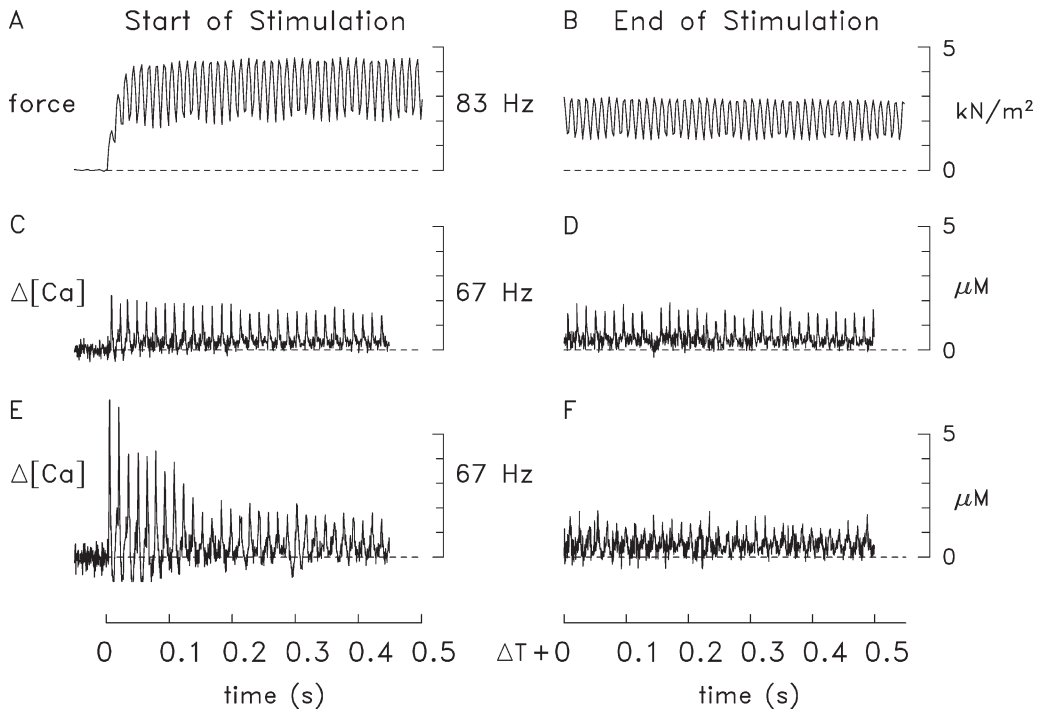

Figure 5. **Examples of force and Δ[Ca^{2+}] measurements from midshipman swimbladder fibers elicited by stimulus trains lasting many seconds.** The labels on the left, middle, and right apply to both sides of the figure. **(A, C, and E)** Examples of force and Δ[Ca^{2+}] responses during the first ~0.5 s of a long stimulus train at the indicated frequency. The trace in E reveals an obvious movement during the first part of the stimulus train. **(B, D, and F)** Responses from the same preparations in A, C, and E but during the last ~0.5 s of stimulation. ΔT denotes the elapsed time between the recording of the traces in A, C, and E versus those in B, D, and F; the ΔT values were 4.3, 9.0, and 9.6 s, respectively. In D and F, the exact elevation of the Δ[Ca^{2+}] traces with respect to the baseline is not known, because data sampling was discontinued while records were stored to disc during the long stimulation period (at ΔT ~3 and ~6 s); thus, for data records after the first, the absolute fluorescence intensity of Mag-fluo-4, and hence the baseline elevation, is uncertain. The elevation of the Δ[Ca^{2+}] traces in D and F has been set, somewhat arbitrarily, at 0.5 μM (see Results). Experiment no. 052114.1 (C and D), 052114.3 (E and F).

in Fig. 5 A, and the response just before cessation of stimulation is shown in Fig. 5 B. Both traces reveal an 83-Hz oscillation that is maintained throughout the stimulus period, as expected for a fiber type that can contribute to continuous sound production by the swimbladder for long time periods. The force oscillation, however, is substantially smaller after some seconds of stimulation.

The traces in Fig. 5 (C–F) show results from two experiments in which Δ[Ca^{2+}] was measured from one fiber in a bundle in response to a 67-Hz stimulus that lasted almost 10 s. The records from the experiment of Fig. 5 (C and D) appear to be largely free of a movement artifact, whereas those from the experiment of Fig. 5 (E and F) contain an obvious movement artifact early in the stimulus train (as indicated by the baseline undershoot of the Δ[Ca^{2+}] trace). After 9 s of stimulation (Fig. 5, D and F), the experiments reveal that (a) each shock in the stimulus train (with the exception of one shock in Fig. 5 D) elicited a distinct peak in the Δ[Ca^{2+}] trace caused by an increment in SR Ca^{2+} release, and (b) the individual Δ[Ca^{2+}] responses are generally similar, with a FDHM of ~1.6 ms and a mean peak of ~1.25 μM above the minimum value.

Overall, these experiments show that midshipman fibers can maintain repetitive AP-evoked releases of SR Ca^{2+} and force responses for many seconds, although the amplitude of the responses may decrease during prolonged stimulation.

Simulation of myoplasmic Ca^{2+} movements during long-lasting high-frequency stimulation

For midshipman fibers stimulated at a high frequency for many seconds, it is of interest to estimate the underlying myoplasmic Ca^{2+} movements, including how much SR Ca^{2+} is released with each AP, how much Ca^{2+} moves onto and off the troponin regulatory sites, and how much Ca^{2+} is returned to the SR by Ca^{2+} pumping. These values are all important for characterizing the performance of swimbladder fibers during the long-lasting calls made by type I males. To estimate these movements, simulations designed to mimic the 67-Hz Δ[Ca^{2+}] measurements shown in Fig. 5 (D and F) (which were recorded at the end of 9 s of continuous stimulation) were performed as described in Materials and methods. The only parameter adjusted in these simulations was the value of *R* in Eq. 3. The value chosen for

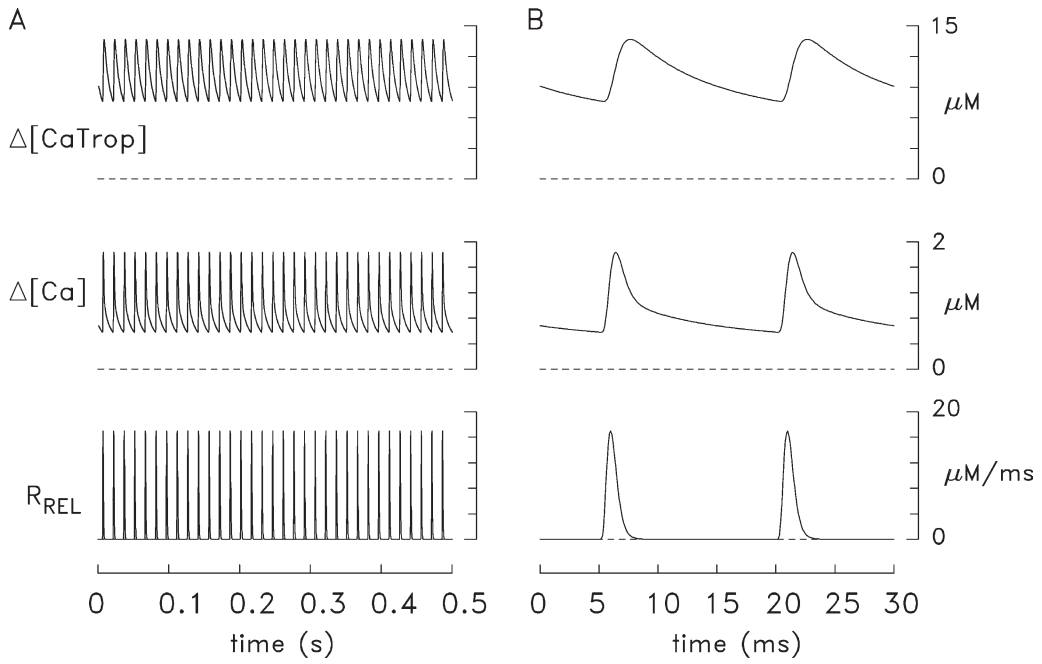

Figure 6. **Simulation results when the midshipman model is driven to steady state with the Ca^{2+} release waveform defined by Eq. 3 repeated at 67 Hz.** The values of *R*, τ1, and τ2 in Eq. 3 were 2,008 μM/ms, 0.8 ms, and 0.32 ms, respectively. The simulated traces are R_{REL} (bottom), Δ[Ca^{2+}] (middle), and Δ[CaTrop] (top); the results for Δ[CaATP], Δ[CaParv], Δ[CaPump], and Δ[CaPumped] (not depicted) are described in the text (see Simulation of myoplasmic Ca^{2+} movements during long-lasting high-frequency stimulation and Simulations with a more-sensitive Ca^{2+} pumping–pCa relation in Results). **(A and B)** In A, the traces are shown on a time base like that on the right side of Fig. 5; in B, two cycles of the traces on the left side are shown on an expanded time base.

R during these long-lasting simulations was that which, at steady-state, elicited individual Δ[Ca^{2+}] responses in the simulated Δ[Ca^{2+}] waveform that had an amplitude of 1.25 μM above the minimum [Ca^{2+}] level—that is, like that observed in Fig. 5 (D and F). Steady state in these simulations was achieved after 2–3 s of calculation (not depicted), similar to the quasi–steady state that was observed in the measurements after ~3 s of stimulation (not depicted).

Fig. 6 shows traces from these simulations. In Fig. 6 A, the 0.5-s time base corresponds to that in Fig. 5 (D and F); that is, the quasi–steady-state response after some seconds of stimulation; in Fig. 6 B, the time base has been expanded to show two cycles of the simulation. The lowermost traces show the R_{REL} waveform. The total Ca^{2+} release in each cycle (not depicted) is 19.8 μM, and the peak R_{REL} is 16.9 μM/ms. The middle traces show Δ[Ca^{2+}], which, as expected, consist of a series of transient oscillations whose peaks are 1.25 μM above the minimum value (which is 0.58 μM). The FDHM of each excursion of Δ[Ca^{2+}] above the minimum value is 1.8 ms, which is close to the mean value observed in the measurements, 1.6 ms (Fig. 5, D and F). The uppermost traces show Δ[CaTrop], which oscillates between minimum and maximum values of 7.6 and 13.7 μM. The difference, 6.1 μM, corresponds to a change in occupancy of 8% of the troponin regulatory sites with each cycle in the stimulus. The FDHM of each oscillation in Δ[CaTrop] above the minimum value is 5.5 ms, which is slightly smaller than the FDHM of Δ[CaTrop] in Fig. 3, 6.4 ms. Overall, there is approximate agreement between the simulated and measured Δ[Ca^{2+}] traces, which supports the conclusion that the Ca^{2+} movements estimated in the simulations are reasonable.

Not depicted in Fig. 6 are the calculated steady-state waveforms of Δ[CaATP], Δ[CaParv], Δ[CaPump], and Δ[CaPumped]. The oscillation in Δ[CaATP] has, as expected, a time course that is virtually identical to that of Δ[Ca^{2+}] but an amplitude that is larger, with minimum and maximum values of 1.8 and 5.8 μM. The Δ[CaParv] and Δ[CaPump] waveforms are nearly constant in each cycle, oscillating between 505.6 and 510.5 μM and between 343.6 and 362.0 μM, respectively. Δ[CaPumped] increases by 19.8 μM during each cycle, the same as the amount of Ca^{2+} released in each cycle, as expected because a steady-state between release and pumping has been reached.

Simulations with a more-sensitive Ca^{2+} pumping–pCa relation

The Ca^{2+} sensitivity of the Ca^{2+} pumping–pCa relation is somewhat higher in the measurements (Fig. 2) than in our standard model of the Ca^{2+} pump (Hollingworth et al., 2006); for example, the pCa at which pumping is half-maximal is ~6.0 in the measurements and ~5.5 in the model. To evaluate the importance of this differ-

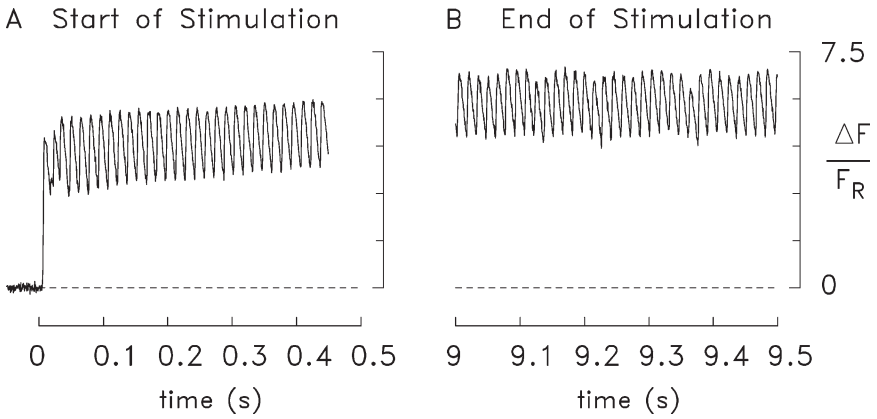

Figure 7. **Δ*F/FR* responses measured from a midshipman swimbladder fiber that was injected with Fluo-4 and excited by a 67-Hz stimulus train that lasted 10 s. (A)** The response during the first part of the recording, which included 0.05 s of baseline plus 0.45 s of stimulation. **(B)** The response during the last part of the recording (9–9.5 s after onset of stimulation).

ence, simulations such as those in Fig. 6 were performed with the Ca^{2+} pumping–pCa relation in the model adjusted to more closely approximate the measurements. A simple empirical way to achieve this is to change the pH in the Ca^{2+} pump reaction scheme from 7.0 to 7.7, which shifts the pCa value for half-maximum pumping to ~6.0 without changing the maximum pumping rate (compare Hollingworth et al., 2006). With this change, 26.9 μM Ca^{2+} release is required in each cycle (36% higher than that in Fig. 6) to give a simulated $\Delta[Ca^{2+}]$ waveform whose amplitude at steady state is 1.25 μM above the minimum value (as in Fig. 6). As expected, a smaller minimum $[Ca^{2+}]$ value is observed in each cycle, 0.30 μM above resting (compared with 0.58 μM in Fig. 6), consistent with the left-shift in the Ca^{2+} pumping–pCa relation. The FDHM of $\Delta[Ca^{2+}]$ with respect to this minimum is 1.5 ms (compared with 1.8 ms in Fig. 6 and 1.6 ms in the measurements). The simulated Δ[CaTrop] waveform oscillates between minimum and maximum values of 4.2 and 10.2 μM (compared with 7.6 and 13.7 μM in Fig. 6), with the amplitude of the excursion being the same, 6.1 μM. The FDHM of each oscillation in Δ[CaTrop] relative to the minimum value is 4.2 ms, which is somewhat briefer than that in Fig. 6, 5.5 ms.

Overall, the differences between these simulations and those in Fig. 6 are not large. The common conclusions that apply to both simulations for a stimulus that continues for several seconds are (a) the amount of SR Ca^{2+} released with each AP is small, in the range 20–27 μM; (b) the minimum value of $[Ca^{2+}]$ during stimulation is 0.3–0.6 μM above the resting level of 0.03 μM, and the mean $[Ca^{2+}]$ during the stimulus (including the resting $[Ca^{2+}]$) is 0.6–0.9 μM; (c) the oscillation in the Δ[CaTrop] waveform is small, ~6 μM, which corresponds to a change in occupancy of the troponin regulatory sites of ~8%; and (d) as expected, the amount of Ca^{2+} pumped during each cycle matches the amount released.

Measurements with Fluo-4 during a long-lasting stimulus

As noted in the preceding section, during a long-lasting high-frequency stimulus, the estimated mean $[Ca^{2+}]$ in the myofibrillar region of a midshipman fiber lies in the range 0.6–0.9 μM. According to the measured Ca^{2+} pumping–pCa relation for midshipman fibers (Fig. 2, black symbols), if mean $[Ca^{2+}]$ is 0.6–0.9 μM, the rate of Ca^{2+} pumping during a long-lasting stimulus is 30–45% of the maximum possible rate. Thus, the Mag-fluo-4 experiments indicate that the rate of Ca^{2+} pumping during a long-lasting stimulus remains comfortably below the maximum possible pumping rate, as would be expected for a stable functional design.

To obtain another experimental estimate of the mean value of free $[Ca^{2+}]$ in a midshipman fiber during a long-lasting stimulus, experiments like those with Mag-fluo-4 were attempted with Fluo-4 (see Materials and methods). Because Fluo-4 is a high-affinity, Ca^{2+}-specific indicator, its $\Delta F/F_R$ signal is expected to be (a) free of interference from $\Delta[Mg^{2+}]$ and (b) of larger amplitude than that of Mag-fluo-4. Thus measurement of Fluo-4's fluorescence change in midshipman fibers, with calibration of its signal in units of $\Delta[Ca^{2+}]$, is expected to provide a check on the quantitative conclusions reached above in the analysis of the Mag-fluo-4 experiments, where the $\Delta[Ca^{2+}]$ measurements are small and somewhat noisy during a long-lasting stimulus. Although only one such experiment in a Fluo-4–injected fiber was successful, that fiber appeared to be a particularly vigorous and healthy one, as it gave robust all-or-nothing responses during the 1.5-h duration of the experiment. Thus, we believe that the results from this fiber are reliable.

Fig. 7 shows sample Fluo-4 recordings from this experiment, in which the fiber was excited by a 67-Hz stimulus train that lasted 10 s. Fig. 7 A shows $\Delta F/F_R$ during the first 0.5 s of recording, and Fig. 7 B shows $\Delta F/F_R$ during the last 0.5 s of recording. The waveforms show that the fiber responded to each shock with an increment of Ca^{2+} release and, after some seconds of continuous stimulation, an apparent steady state was reached in which Ca^{2+} release and Ca^{2+} pumping were in balance. As expected, the amplitude of the Fluo-4 $\Delta F/F_R$ signal is much larger (~10-fold) than that of the Mag-fluo-4 signal (Fig. 1; see also Fig. 5).

From the mean value of $\Delta F/F_R$ in Fig. 7 B, 5.90, and the relation between $[Ca^{2+}]$ and Fluo-4's fluorescence estimated previously for the myoplasm (Nelson et al., 2014), the mean value of $[Ca^{2+}]$ in the myofibrillar region of the fiber during the period 9–9.5 s is calculated to be 0.39 µM. This estimate depends on the value assumed for resting $[Ca^{2+}]$, 0.03 µM (Table 1), which is not well known in the experiments. If, for example, resting $[Ca^{2+}]$ is assumed to be 0.06 µM, a value that is thought to be an upper limit of resting $[Ca^{2+}]$ in intact frog skeletal muscle fibers (e.g., Hollingworth et al., 2001), the mean $\Delta F/F_R$ value of 5.90 in Fig. 7 B calibrates to a mean value of $[Ca^{2+}]$ of 0.69 µM. If resting $[Ca^{2+}]$ were as high as 0.09 µM, which may be considered unlikely, the $\Delta F/F_R$ value of 5.90 calibrates to a mean $[Ca^{2+}]$ in the myofibrillar region of 1.1 µM.

The main conclusion from this Fluo-4 experiment is that the mean $[Ca^{2+}]$ level during a long-lasting high-frequency stimulus is likely to fall in the range 0.4–1.1 µM. This is in satisfactory agreement with the range 0.6–0.9 µM estimated in the Mag-fluo-4 experiments and simulations. Thus, this Fluo-4 experiment supports the conclusion of the Mag-fluo-4 experiments, that the rate of Ca^{2+} pumping during a long-lasting stimulus likely remains well below the maximal possible pumping rate.

DISCUSSION

How midshipman swimbladder muscle pumps calcium during calling

We hypothesized two possibilities for how midshipman fibers handle Ca^{2+} during its 100%-duty-cycle call. First, they could have an exceptionally fast Ca^{2+} pumping ability. Our skinned fiber studies (Fig. 2), however, demonstrate that the maximum pumping rate per kilogram wet weight is actually lower than in toadfish (Young et al., 2003). Second, they could release only a small amount of Ca^{2+}, either with each stimulus if the muscle is synchronous or averaged over several contractions if the muscle is asynchronous. The midshipman muscle has a well-defined twitch response, suggesting that the muscle is synchronous. Indeed, our measurements show that the fiber is capable of responding to a high-frequency stimulus (67–100 Hz) with an individual fiber contraction and release of Ca^{2+} linked to each stimulus. Our measurements further show that a balance between Ca^{2+} release and pumping is readily achieved in midshipman fibers during maintained activity. Although baseline $[Ca^{2+}]$ goes up with the first seconds of contraction (e.g., Fig. 1 F), it later remains approximately constant (Fig. 5, D and F; and Fig. 7 B), indicative of such a balance.

Our analyses show that the amount of Ca^{2+} released per stimulus in midshipman swimbladder fibers is quite small, particularly compared with toadfish fibers. With a single twitch, the amount of Ca^{2+} released into the myofibrillar region of the fiber is estimated to be about eightfold smaller in midshipman than in toadfish, and a similar reduction applies to later stimuli in a high-frequency train (Figs. 5 and 6; Harwood et al., 2011). The total Ca^{2+} released with the first AP (110–120 µM) compares with the following values in other fiber types that we have examined: toadfish swimbladder, 750 µM (Harwood et al., 2011); mouse fast-twitch, 350 µM (Baylor and Hollingworth, 2003); mouse slow-twitch, 110 µM (Baylor and Hollingworth, 2003).

Our measurements show that the SR Ca^{2+} pumps in midshipman have a large reserve capacity during normal maintained activity. The maximum ATP utilization of the Ca^{2+} pumps (Fig. 2) is ∼700 µmol/kg wet weight of muscle/s, which is equivalent to 1,400 µmol/kg/s of pumped Ca^{2+}. Our model simulations (Fig. 5 and related) show that, after several seconds of prolonged activity, the Ca^{2+} release per stimulus is between 20 and 27 µM (concentration units referring to the myofibrillar water volume), which is equivalent to 3.1–4.2 µmol Ca^{2+}/kg wet weight. At 67 Hz, the Ca^{2+} release would be 208–281 µmol/kg/s, and the SR Ca^{2+} pumping would be the same value. This is ∼15–20% of the maximum rate of SR Ca^{2+} pumping measured in skinned midshipman fibers. With 100-Hz stimulation, there would still be sufficient excess pump capacity to pump all the released Ca^{2+} if the release per stimulus remained the same as at 67 Hz. However, it is likely that the Ca^{2+} release per stimulus would be smaller at 100 Hz as a result of an increase in the degree of Ca^{2+}-dependent inactivation of the Ca^{2+} release channels because the time between stimuli for recovery from inactivation would be shorter.

Thus, the key element that permits Ca^{2+} pumping in midshipman swimbladder muscle to keep up with Ca^{2+} releases for long periods of high-frequency stimulation is the small Ca^{2+} release per stimulus. Several possible mechanisms might underlie the markedly reduced Ca^{2+} release per stimulus compared with toadfish fibers. These include (a) a less effective coupling mechanism between the voltage sensors of the transverse tubules (dihydropyridine receptors [DHPRs]) and the SR Ca^{2+} release channels (ryanodine receptors [RyRs]), (b) a smaller number of DHPR:RyR units per unit myofibrillar volume, (c) a more rapid onset and slower relief of Ca^{2+} inactivation of Ca^{2+} release, and (d) an SR that is less loaded with Ca^{2+}. Additional experiments will be required to investigate the relative importance of these possibilities.

The small Ca^{2+} release of midshipman is necessary not only for Ca^{2+} pumping to keep up in real time but also to maintain a reasonable energy budget. The time-averaged Ca^{2+} release for toadfish, which make intermittent calls all night, can be estimated from Nelson et al. (2014) (Fig. 8b, call period 10.5 s). Subsequent to the initial call, 0.5-s calls release 1.72 mmol Ca^{2+}/kg wet weight. This corresponds to a time-averaged release

of 164 μmol/kg/s. Hence, even though midshipman have ~20-fold larger duty cycles than toadfish (100% vs. 3–8%), the time-averaged Ca^{2+} release during calling (and therefore the required Ca^{2+}pumping) is less than twofold greater (208–281 μmol/kg/s) than in toadfish. Thus, the small Ca^{2+} release in midshipman obviously reduces the metabolic cost of calling.

In midshipman, the SR Ca^{2+} pumps likely work at a nearly constant rate throughout calling. The underlying mechanism for this constancy is that the Ca^{2+} pump turnover rate is very slow (with a period of hundreds of milliseconds at 16°C) compared with the frequency of simulation (and hence to the releases of Ca^{2+}, period of 10–20 ms). For instance, after several seconds of stimulation, the estimated concentration of Ca^{2+} bound to the pump becomes approximately constant with fluctuations of less than 5% (see Results) in response to individual stimuli (Fig. 3 A). The slow pump reaction kinetics essentially filters the high-frequency changes in [Ca^{2+}] so that the pump rate is roughly predictable from the relation in Fig. 2 and the mean [Ca^{2+}] during activity. Another critical design feature that is associated with this steady Ca^{2+} pumping during activity is the higher Ca^{2+} sensitivity for pumping compared with force generation (Fig. 2). Mean [Ca^{2+}] can be relatively high, up to 1 μM, which is sufficient to activate the Ca^{2+} pumps at roughly half the maximal level, yet be well below the threshold for significant force generation, thus permitting some fiber relaxation between stimuli.

Ca^{2+} pumping in other cell types during repetitive motor activities

This study is one of only a few cases in which Ca^{2+} release and reuptake have been quantitatively estimated during the naturally occurring stimulation pattern. With midshipman, this pattern could be estimated based on the recording of sound pulses by hydrophone from a remote location, which shows that there is a 1:1 relationship between sound pulses and stimuli (Elemans et al., 2014). In contrast, many studies of muscle Ca^{2+} movements rely on fiber activation by means of single twitches or a brief tetanus applied in isolation, an activity that is not representative of the repetitive motor movements common to many forms of locomotion and sound production. Because it takes considerable time for the SR to resequester all the released Ca^{2+} (see, e.g., the Discussion in Nelson et al., 2014), if mean [Ca^{2+}] is not high and Ca^{2+} release per stimulus is not low, it is unlikely that sufficient time will be available for Ca^{2+} pumping to match Ca^{2+} release during a period of brief activity. Although midshipman swimbladder muscle represents an extreme case of constant stimulation at a high frequency (70–100 stimulations/s at 15°C for an hour), the concept of Ca^{2+} pumping at a steady rate throughout motor activity may be a more general phenomenon. During many types of naturally occurring maintained activities, baseline [Ca^{2+}] may rise progressively to a steady state—and also, therefore, the mean rate of Ca^{2+} pumping. For example, during high-frequency wing beats of small birds (up to 70 Hz), it is unlikely that at the onset of activity there will be time to pump all the Ca^{2+} back to the SR between wing beats. Thus, a slow buildup of baseline [Ca^{2+}] to a steady level is expected during continued activity. Testing of this theory would require (1) determination of the stimulation pattern of the muscle fiber type used during normal activity and (2) recording Ca^{2+} transients (both low- and high-affinity dyes, as in the current study) from fibers driven under the in vivo stimulation pattern.

Further studies

In this first physiological study on midshipman swimbladder muscle, we leveraged the physiological information garnered over the past two decades on toadfish swimbladder muscle function to focus our experiments on Ca^{2+} movements. Several further studies on midshipman should be pursued to further improve our understanding of the design of this extreme muscle. One limitation of the present study is that we do not have biochemical evidence concerning whether there are one or two Ca^{2+} activation sites on Troponin-C (TNC). Our modeling indicates that this uncertainty has relatively small quantitative effect on the values of Ca^{2+} release obtained and does not affect the overall conclusion. Nonetheless, to obtain more precise values, biochemical studies would be very useful.

We can further increase the precision of this Ca^{2+} release estimate by using an independent energetic approach that does not involve assumptions on the concentrations and kinetics of Ca^{2+} binding reactions. We previously showed on toadfish swimbladder (Harwood et al., 2011) that, when measured over a sufficient time, recovery O_2 consumption (ΔO_2) in the presence of BTS provides an accurate measure of how much Ca^{2+} was pumped back into the SR, which is equal to the amount of Ca^{2+} that was released during the contractions studied. In toadfish, this approach provided very similar results (within 10%) to values obtained by measuring Ca^{2+} transients and modeling Ca^{2+} release, as we have used in this study (Harwood et al., 2011).

Further, measurements in the presence and absence of BTS permit the determination of the total energy used by midshipman swimbladder muscle to power calling, and the proportion of the energy that is used by the Ca^{2+} pumps and the cross-bridges. Because midshipman swimbladder muscles generate more muscle contractions in an hour than any other known muscle, understanding its energetics may provide additional insights into the constraints under which this unique muscle has evolved.

As mentioned earlier, the force generated by the muscle per cross section is very low because of the relatively

low cross section of myofilaments caused by the large space taken up by SR and mitochondria. We also anticipate that the power generation is very low. In addition to the low force, the reduction of sarcomeres in series for a given length of fiber (because of elongated Z-bands), would reduce the velocity as well. It would therefore be of considerable interest to determine the power generation as a function of frequency with the workloop technique in midshipman swimbladder as we have in toadfish (Young and Rome, 2001).

How midshipman swimbladder fibers produce mechanical work for sound production

Perhaps the most compelling remaining question is how the relatively modest fluctuations in troponin occupancy estimated in midshipman fibers with each stimulus permit useful mechanical work to be done. As stated, it is very unlikely that midshipman swimbladder fibers are asynchronous. However, midshipman have two unusual features that may be important in explaining how sound can be produced with relatively small changes in troponin occupancy. First, the swimbladder fibers of calling midshipman have greatly enlarged Z-bands (Bass and Marchaterre, 1989; Brantley et al., 1993; Lewis et al., 2003). The width of the Z-bands in the swimbladder muscles of calling males (type 1) is ∼1.0–1.2 µm whereas all the other midshipman muscles, including the swimbladders of females and type 2 males, have typical Z-band widths of 0.05 µm (Bass and Marchaterre, 1989), as also occurs in toadfish fibers. Second, it has been recently noted that during calling, male midshipman hyperinflate their swimbladder (Bass et al., 2015). The possibility exists that hyperinflation permits the swimbladder to become a resonant structure. If so, the extra elasticity afforded by the unusually long Z-bands might promote shortening deactivation and stretch activation as the swimbladder vibrates, permitting mechanical work to be done. Further studies on midshipman swimbladder muscle mechanics and bladder–muscle interactions are necessary to determine the importance of these processes.

ACKNOWLEDGMENTS

The authors dedicate this paper to the memory of R.K. Josephson, a pioneer in the field of high-frequency muscle action, and to the memory of Prof. R. McNeill Alexander FRS, the father of modern biomechanics who studied swimbladders early on and was a friend and mentor to L.C. Rome.

We thank Dr. Andrew Bass for helpful discussions concerning the anatomy of midshipman swimbladder fibers.

This work was supported by a grant to L.C. Rome from the National Science Foundation (IOS-1145981).

The authors declare no competing financial interests.

Author contributions: All authors were involved in conceptualization, experimentation, and writing.

Eduardo Ríos served as editor.

Submitted: 21 January 2017
Revised: 24 July 2017
Accepted: 22 November 2017

REFERENCES

Appelt, D., V. Shen, and C. Franzini-Armstrong. 1991. Quantitation of Ca ATPase, feet and mitochondria in superfast muscle fibres from the toadfish, Opsanus tau. *J. Muscle Res. Cell Motil.* 12:543–552. https://doi.org/10.1007/BF01738442

Bass, A.H., and M.A. Marchaterre. 1989. Sound-generating (sonic) motor system in a teleost fish (*Porichthys notatus*): Sexual polymorphism in the ultrastructure of myofibrils. *J. Comp. Neurol.* 286:141–153. https://doi.org/10.1002/cne.902860202

Bass, A.H., D.A. Bodnar, and M.A. Marchaterre. 1999. Complementary explanations for existing phenotypes in an acoustic communication system. *In* Neural Mechanisms of Communication. M. Hauser, and M. Konishi, editors. MIT Press, Cambridge, MA, 493–514.

Bass, A.H., B.P. Chagnaud, and N. Feng. 2015. Comparative neurobiology of sound production in fishes. *In* Sound Communication in Fishes, Animal Signals and Communication. Vol. 4. F. Ladich, editor. Springer-Verlag, Vienna, Austria. 35–75.

Baylor, S.M., and S. Hollingworth. 2003. Sarcoplasmic reticulum calcium release compared in slow-twitch and fast-twitch fibres of mouse muscle. *J. Physiol.* 551:125–138. https://doi.org/10.1113/jphysiol.2003.041608

Baylor, S.M., W.K. Chandler, and M.W. Marshall. 1983. Sarcoplasmic reticulum calcium release in frog skeletal muscle fibres estimated from Arsenazo III calcium transients. *J. Physiol.* 344:625–666. https://doi.org/10.1113/jphysiol.1983.sp014959

Brantley, R.K., J. Tseng, and A.H. Bass. 1993. The ontogeny of inter- and intrasexual vocal muscle dimorphisms in a sound-producing fish. *Brain Behav. Evol.* 42:336–349. https://doi.org/10.1159/000114170

Cheung, A., J.A. Dantzig, S. Hollingworth, S.M. Baylor, Y.E. Goldman, T.J. Mitchison, and A.F. Straight. 2002. A small-molecule inhibitor of skeletal muscle myosin II. *Nat. Cell Biol.* 4:83–88. https://doi.org/10.1038/ncb734

Edds-Walton, P., L. Mangiamele, and L.C. Rome. 2002. Boatwhistles from osyter toadfish (*Opsanus tau*) around Waquoit Bay, Massachsetts. *J. Bioacoustics.* 13:153–173. https://doi.org/10.1080/09524622.2002.9753493

Elemans, CPH, AF Mensinger, and LC Rome. 2014. Vocal production complexity correlates with neural instructions in the oyster toadfish (Opsanus tau). *J. Exp. Biol.* 217:1887–1893. https://doi.org/doi: 10.1242/jeb.097444

Harwood, C.L., I.S. Young, B.A. Tikunov, S. Hollingworth, S.M. Baylor, and L.C. Rome. 2011. Paying the piper: The cost of Ca^{2+} pumping during the mating call of toadfish. *J. Physiol.* 589:5467–5484. https://doi.org/10.1113/jphysiol.2011.211979

Hollingworth, S., J. Peet, W.K. Chandler, and S.M. Baylor. 2001. Calcium sparks in intact skeletal muscle fibers of the frog. *J. Gen. Physiol.* 118:653–678. https://doi.org/10.1085/jgp.118.6.653

Hollingworth, S., W.K. Chandler, and S.M. Baylor. 2006. Effects of tetracaine on voltage-activated calcium sparks in frog intact skeletal muscle fibers. *J. Gen. Physiol.* 127:291–307. https://doi.org/10.1085/jgp.200509477

Hollingworth, S., K.R. Gee, and S.M. Baylor. 2009. Low-affinity Ca^{2+} indicators compared in measurements of skeletal muscle Ca^{2+} transients. *Biophys. J.* 97:1864–1872. https://doi.org/10.1016/j.bpj.2009.07.021

Josephson, R.K., J.G. Malamud, and D.R. Stokes. 2000. Asynchronous muscle: a primer. *J. Exp. Biol.* 203:2713–2722.

Konishi, M., S. Hollingworth, A.B. Harkins, and S.M. Baylor. 1991. Myoplasmic calcium transients in intact frog skeletal muscle

fibers monitored with the fluorescent indicator furaptra. *J. Gen. Physiol.* 97:271–301. https://doi.org/10.1085/jgp.97.2.271

Konishi, M., N. Suda, and S. Kurihara. 1993. Fluorescence signals from the Mg^{2+}/Ca^{2+} indicator furaptra in frog skeletal muscle fibers. *Biophys. J.* 64:223–239. https://doi.org/10.1016/S0006-3495(93)81359-6

Launikonis, B.S., and D.G. Stephenson. 1997. Effect of saponin treatment on the sarcoplasmic reticulum of rat, cane toad and crustacean (yabby) skeletal muscle. *J. Physiol.* 504:425–437. https://doi.org/10.1111/j.1469-7793.1997.425be.x

Lewis, M.K., P.C. Nahirney, V. Chen, B.B. Adhikari, J. Wright, M.K. Reedy, A.H. Bass, and K. Wang. 2003. Concentric intermediate filament lattice links to specialized Z-band junctional complexes in sonic muscle fibers of the type I male midshipman fish. *J. Struct. Biol.* 143:56–71. https://doi.org/10.1016/S1047-8477(03)00121-7

Nelson, F.E., S. Hollingworth, L.C. Rome, and S.M. Baylor. 2014. Intracellular calcium movements during relaxation and recovery of superfast muscle fibers of the toadfish swimbladder. *J. Gen. Physiol.* 143:605–620. https://doi.org/10.1085/jgp.201411160

Rome, L.C. 2006. Design and function of superfast muscles: New insights into the physiology of skeletal muscle. *Annu. Rev. Physiol.* 68:193–221. https://doi.org/10.1146/annurev.physiol.68.040104.105418

Rome, L.C., and A.A. Klimov. 2000. Superfast contractions without superfast energetics: ATP usage by SR-Ca2+ pumps and crossbridges in toadfish swimbladder muscle. *J. Physiol.* 526:279–286. https://doi.org/10.1111/j.1469-7793.2000.t01-1-00279.x

Rome, L.C., and S.L. Lindstedt. 1998. The quest for speed: Muscles built for high frequency contractions. *News Physiol. Sci.* 13:261–268.

Rome, L.C., A.A. Sosnicki, and D.O. Goble. 1990. Maximum velocity of shortening of three fibre types from horse soleus muscle: Implications for scaling with body size. *J. Physiol.* 431:173–185. https://doi.org/10.1113/jphysiol.1990.sp018325

Rome, L.C., D.A. Syme, S. Hollingworth, S.L. Lindstedt, and S.M. Baylor. 1996. The whistle and the rattle: The design of sound producing muscles. *Proc. Natl. Acad. Sci. USA.* 93:8095–8100. https://doi.org/10.1073/pnas.93.15.8095

Rome, L.C., C. Cook, D. Syme, M. Connaughton, M. Ashley-Ross, A.A. Klimov, B. Tikunov, and Y.E. Goldman. 1999a. Trading force for speed: Why superfast crossbridge kinetics leads to superlow forces. *Proc. Natl. Acad. Sci. USA.* 96:5826–5831. https://doi.org/10.1073/pnas.96.10.5826

Rome, L.C., A.A. Klimov, and I.S. Young. 1999b. A new approach for measuring real-time calcium pumping and SR function in muscle fibers. *Biol. Bull.* 197:227–228. https://doi.org/10.2307/1542618

Stienen, G.J.M., R. Zaremba, and G. Elzinga. 1995. ATP utilization for calcium uptake and force production in skinned muscle fibres of Xenopus laevis. *J. Physiol.* 482:109–122. https://doi.org/10.1113/jphysiol.1995.sp020503

Tikunov, B.A., and L.C. Rome. 2009. Is high concentration of parvalbumin a requirement for superfast relaxation? *J. Muscle Res. Cell Motil.* 30:57–65. https://doi.org/10.1007/s10974-009-9175-z

Young, I.S., and L.C. Rome. 2001. Mutually exclusive muscle designs: The power output of the locomotory and sonic muscles of the oyster toadfish (Opsanus tau). *Proc. Biol. Sci.* 268:1965–1970. https://doi.org/10.1098/rspb.2001.1731

Young, I.S., C.L. Harwood, and L.C. Rome. 2003. Cross-bridge blocker BTS permits direct measurement of SR Ca2+ pump ATP utilization in toadfish swimbladder muscle fibers. *Am. J. Physiol. Cell Physiol.* 285:C781–C787. https://doi.org/10.1152/ajpcell.00025.2003